Indian Journal of Pharmaceutical Education and Research

Initial draft · Author queries

Manuscript: IJPER-2026-0219 · **Version:** V5 · **Date:** 06 Nov 2026, 14:43 IST

Title: Development and Optimization of an Apigenin-Loaded Silver Nanoparticle Gel for Enhanced Topical Delivery of Apigenin

Author queries

Please also check (2)

> References never cited in text: [41, 53]

> Correspondence author 'Mohammed Albratty' has no salutation (Dr./Prof./Mr./Ms./Mrs.).

How to answer: every query is numbered (AQ1, AQ2 …) and the yellow AQ tags in the margin of the proof show where it applies (the page is given after each query). Open the review link from our e-mail, answer each query and mark your corrections directly on the proof, or upload a corrected Word file, then press Submit. If everything is correct, choose Accept. Please do not change the layout - only corrections to the text.

INITIAL DRAFT · V5 · 06 Nov 2026, 14:43 IST

Ind. J. Pharm. Edu. Res., 2027; 1-15.
https://www.ijper.org

Original Article

Development and Optimization of an Apigenin-Loaded Silver Nanoparticle Gel for Enhanced Topical Delivery of Apigenin

Hafiz A. Makeen[1], Mohammed Albratty[2,*]

[1]Pharmacy Practice Research Unit, Department of Clinical Pharmacy, College of Pharmacy, Jazan University, Jazan, SAUDI ARABIA.
[2]Department of Pharmaceutical Chemistry and Pharmacognosy, College of Pharmacy, Jazan University, Jazan, SAUDI ARABIA.

ABSTRACT

Background: Apigenin, a naturally occurring flavonoid with potent anti-inflammatory and antioxidant properties, has limited topical efficacy because of its low skin permeability and poor water solubility. **Objectives:** This study aimed to develop and optimize an Apigenin-Loaded Silver Nanoparticle Gel (APG-AgNP gel) to enhance the topical delivery of apigenin. **Materialsd and Methodos:** The microwave-assisted synthesis of APG-AgNPs was optimised using a Box-Behnken design. For the optimised nanoparticles, measurements were made of particle size, Polydispersity Index (PDI), zeta potential, shape, entrapment efficiency, *in vitro* drug release, and antioxidant activity. Confocal Laser Scanning Microscopy (CLSM), stability, dermatokinetic behaviour, spreadability, texture, and *ex vivo* skin penetration were all evaluated after the optimized formulation was incorporated into a topical gel. **Results:** The optimised APG-AgNPs showed good stability and sustained release properties with a particle size of 182.32 nm, PDI of 0.244, zeta potential of -34.29 mV, entrapment efficiency of 88.98%, and cumulative drug release of 80.44±3.99%. Compared to the traditional apigenin solution, the formulation exhibited higher antioxidant activity (82.26%). CLSM showed deeper skin penetration, while dermatokinetic analysis demonstrated greater apigenin deposition in the epidermis and dermis than the conventional gel. No major changes were observed in the measured physicochemical characteristics during storage. **Conclusion:** The optimized APG-AgNP gel enhanced the release, skin penetration and cutaneous deposition of apigenin, suggesting its potential for topical apigenin delivery. However, its topical safety and potential application in psoriasis need to be confirmed in appropriate *in vivo* studies.

Keywords: Antioxidant activity, Apigenin, Dermatokinetic study, Psoriasis, Silver nanoparticles, Topical gel.

Correspondence:
Prof. Mohammed Albratty
Department of Pharmaceutical Chemistry and Pharmacognosy, College of Pharmacy, Jazan University, Jazan-45142, SAUDI ARABIA.
Email: malbratty@jazanu.edu.sa

Received: 09-07-2026;
Revised: 11-09-2026;
Accepted: 27-10-2026.

www.ijper.org

INTRODUCTION

Psoriasis is a prevalent medical condition that is classified as a chronic autoimmune inflammatory disorder caused by excessive proliferation of keratinocytes and impaired differentiation affecting the skin.[1] Furthermore, Th17 cells and associated inflammatory cytokines, including IL-23, contribute to the pathogenesis of psoriasis.[2] The findings of the World Health Organization (WHO) indicated that the frequency of this condition ranges from 1.5% to 5% in underdeveloped countries and from 0.9% to 11.4% globally.[3] The ailment typically occurs with the occurrence of scaly lesions which can be found in many areas of the body, commonly affecting the scalp and joints. The distribution of these lesion's changes depending on seriousness of the ailment.[4] It has been observed that individuals afflicted with psoriatic arthritis exhibit an upsurge in the susceptibility to the development of cutaneous psoriasis.[5] Therapeutic interventions currently in existence provide significant relief in managing symptoms associated with the disease; however, they do not address the underlying etiology and are accompanied by unfavorable side effects.[6]

Flavonoids, a group of naturally occurring compounds distinguished by their varied phenolic structures, are present in an extensive range of sources such as tea, grains, wine, fruits, roots, bark, vegetables, stems and flowers. These features are ascribed to their ability to provide anti-carcinogenic effects, anti-inflammatory, antioxidative and, anti-mutagenic action, in addition to their capability to regulate the operation of crucial cellular enzymes.[7]

DOI: 10.5530/ijper.20270219

Copyright Information :
Copyright Author (s) 2027 Distributed under Creative Commons CC-BY 4.0

Publishing Partner : Manuscript Technomedia. [www.mstechnomedia.com]

Apigenin (APG) (4',5,7- trihydroxyflavone) is a flavone compound that possesses notable anti-inflammatory and antioxidant characteristics. Apigenin has been shown to have the ability to reduce the tumorigenic response of skin malignancies as well as skin inflammatory diseases such atopic dermatitis, pruritus, and psoriasis.[8] It effectively suppresses the NF-kB activity and reduces the transactivation of the luciferase reporter gene induced by TNF. Additionally, apigenin exhibits the ability to decrease TNF levels, suppress the expression of COX-2, IL-6, and IL-8, and inhibit the transactivation of the luciferase reporter gene induced by TNF.[8,9] However, the limited water solubility of the active apigenin imposes restrictions on its clinical application. The aqueous solubility of apigenin is restricted to a maximum of 0.0032 mg/mL, hence imposing constraints on its oral bioavailability. By using a different administration mechanism and selecting an appropriate dosage formulation, the challenges related to the oral bioavailability of APG can be overcome.[10]

In recent decades, the topic of nanotechnology has garnered significant attention from academics across several disciplines, mainly in the realm of drug delivery.[11] The utilization of nanotechnology offers several advantages in contrast to conventional methods of drug delivery. The benefits encompass the capacity to modify the solubility of hydrophobic compounds, attain regulated or prolonged release of pharmaceuticals, improve the stability of drugs, and enable targeted therapy directed towards specific locations of action. These advantages ultimately lead to increased effectiveness and reduced adverse effects. A variety of nanocarriers were utilized in the context of topical drug administration, encompassing polymeric, lipidic, and metallic formulations.[12]

Metallic nanoparticles have a significant role in drug delivery, when it comes to identifying the most efficient pharmaceuticals with certain properties.[13] The utilization of nanoparticles promotes the permeation of drugs into the dermal layer, hence augmenting their antimitotic, anti-inflammatory, and antibacterial characteristics.[14] The exploitation of APG for the development of Silver Nanoparticles (AgNPs) by microwave method. Multiple studies have provided evidence of the notable inhibitory impact of AgNPs on microorganisms,[15] in addition to their ability to scavenge free radicals and exhibit anti-inflammatory effects.[16,17]

The goal of current research was to design APG encapsulated silver nanoparticles and construct a carbopol 940 gel, to improve the efficacy of APG when applied topically. The study employed the Box-Behnken Design (BBD) to formulate and optimize silver nanoparticles including APG. Ultimately, the obtained preparation was further evaluated for a range of physical characteristics and various other parameters. The present study aimed to develop and optimize an apigenin-loaded silver nanoparticle gel and evaluate its physicochemical properties, drug release, antioxidant activity, *ex vivo* skin permeation and dermatokinetic behaviour. The formulation was designed to enhance the topical delivery and skin deposition of apigenin for its potential application in psoriasis. However, the study focused on formulation performance and topical delivery; psoriasis-specific efficacy and topical safety were not directly evaluated.

MATERIALS AND METHODS

Sigma-Aldrich, St. Louis, MO, USA, provided the apigenin and silver nitrate. Triethanolamine (TEA), HPLC-grade methanol and Polyethylene Glycol-400 (PEG) were procured from S.D. Fine Chemicals Ltd., The acquisition of rat rodent skin was made through Esty Pvt. Ltd., India. B.S. Goodrich, a reputable Cleveland-based supplier, provided the Carbopol-940 polymer.

Apigenin loaded silver nanoparticles

The apigenin solution was combined including 10 mM Silver Nitrate ($AgNO_3$) solution under constant stirring at room temperature to produce the APG-AgNP. Subsequently, the solution underwent microwave irradiation operating at a constant 2.45 GHz of frequency within a given temperature limit of 90°C. It was observed that the solution saw a noticeable shift in color, transitioning from a transparent state to a deep shade of brown. The observed change in color indicated the occurrence of silver nanoparticle creation, a phenomenon that was afterwards verified by the utilization of UV spectroscopy. The spectroscopic analysis unveiled a lambda max value exceeding 400 nm. After undergoing centrifugation, the silver nanoparticles were exposed to a cleaning method including the use of acetone and distilled water to eliminate any particles that are soluble in water. The powdered nanoparticles were characterized to make sure that the process of making them was accurate.[18]

Silver nanoparticles: Optimization

The APG-AgNP formulation was optimized using a Box-Behnken design generated with Design-Expert version 13 (Stat-Ease Inc., USA). The independent variables were $AgNO_3$ concentration (A: 5, 10 and 15 mM), APG concentration (B: 5, 10 and 15 mg) and microwave power (C: 200, 400 and 600 W). These levels were coded as low (-1), medium (0) and high (+1), respectively, as presented in Table 1. Particle size (Y_1, nm) and absorbance (Y_2) were selected as the response variables. Particle size was minimized to obtain nanometric particles, whereas absorbance at the surface-plasmon-resonance wavelength was maximized as an indicator of AgNP formation. Particle size was minimized to obtain nanometric particles suitable for topical delivery, whereas absorbance at the surface-plasmon-resonance wavelength was maximized as an indirect indicator of AgNP formation. However, absorbance was interpreted together with particle size, PDI, zeta potential and TEM findings because absorbance alone does not establish nanoparticle size, purity or stability. The design

INPRESS

www.ijper.org

generated 17 experimental runs, including five centre-point runs, as shown in Table 2. The experimental data were fitted to different polynomial models and analysed using ANOVA. Model selection was based on model significance, lack of fit, R^2, adjusted R^2, predicted R^2, coefficient of variation and adequate precision. A second-order polynomial equation was generated through multiple-regression analysis to describe the relationship between the independent variables and each response. Numerical optimization was subsequently performed by minimizing particle size and maximizing absorbance using the overall desirability function.[19]

Characterization of optimized silver nanoparticles

UV spectroscopy

UV-visible spectroscopy is a highly valuable method employed for the first representation of produced nanoparticles. Additionally, it serves as a means to monitor the synthesis process and assess the stability of AgNP.[20] Silver nanoparticles possess distinctive optical characteristics that result in their pronounced interaction with particular wavelengths of light.[20] The silver nanoparticles was proven to have been successful after a measurement of the Surface Plasmon Resonance (SPR) that was exhibited by the colloidal solution.[21] A Shimadzu UV-vis spectrophotometer (Kyoto, Japan) was used for analyzing the spectra in the 300-850 nm wavelength range.

Particle size, PDI and zeta potential

Zetasizer Nano ZS (Malvern Instruments Ltd., Worcestershire, UK), Dynamic Light Scattering (DLS) were used to examine the mean particle size, Polydispersity Index (PDI), and surface charge of the optimised apigenin-loaded silver nanoparticles (Opt-APG-AgNPs). To guarantee precise light scattering analysis, the nanoparticle suspension was diluted 100 times with deionised water prior to measurement. To ensure reproducibility, all tests were conducted in triplicate and measurements were made at 25±2°C with a scattering angle of 90°.[22]

Table 1: Independent and dependent variables of APG-AgNP for BBD.

Variables		Level used		
Independent factors		**(-1)**	**(0)**	**(+1)**
A = Conc. of $AgNO_3$(mM)		05	10	15
B = Drug conc. (mg)		05	10	15
C = microwave power (watt)		200	400	600
Responses		**Aim**		
Y_1= Particle size (nm)		Minimize		
Y_2= Absorbance		Maximize		

Entrapment efficiency

By removing the unencapsulated medication from the nanoparticle dispersion using chilled centrifugation (SIGMA 3-30 K, Steinheim, Germany), the entrapment effectiveness of the optimised apigenin-loaded silver nanoparticles (Opt-APG-AgNPs) was assessed. The nanoparticle pellet was obtained by centrifuging the formulation for 3 hr at 4±1°C at 15,000 rpm. To guarantee full extraction of the encapsulated medication, the pellet containing the entrapped apigenin was gathered and broken apart using methanol. To create a homogenous dispersion, the resultant solution was diluted in a 1:9 (v/v) ratio with Phosphate-Buffered Saline (PBS, pH 7.4) and sonicated for 5 min. A UV-visible spectrophotometer (Shimadzu UV-1800, Tokyo, Japan) was used to measure the amount of apigenin in an aliquot (1 mL) of the sample after it had been suitably diluted with PBS (pH 7.4) at 270 nm. The following formula was used to determine the %EE.[23]

$$\% \text{ EE} = \frac{\text{Total amount of APG entrapped}}{\text{Total amount of APG added}} \times 100$$

Transmission electron microscopy (TEM)

TEM instrument (Morgagni 268D, FEI, Eindhoven, The Netherlands) with an accelerating voltage of 15 kV was used to analyse the surface morphology and structural features of the optimised apigenin-loaded silver nanoparticles (Opt-APG-AgNPs). The sample was prepared by carefully placing 10-20 µL of the nanoparticle dispersion onto a copper grid covered with carbon and letting it adsorb for a few minutes. To improve picture contrast, the sample was subsequently negatively stained for 10 sec using 1% (w/v) phosphotungstic acid. Before imaging, the grid was allowed to air dry at room temperature after any excess stain was carefully removed using filter paper. The generated grids were then examined using TEM micrographs to ascertain the size, distribution, and shape of the particles.[24]

Drug release

The dialysis bag diffusion method was used to assess the *in vitro* release of APG from the optimised apigenin-loaded silver nanoparticles (Opt-APG-AgNPs). Before being used, a 12 kDa MWCO dialysis membrane (Sigma-Aldrich, St. Louis, MO, USA) was hydrated in distilled water for a whole day. Separate dialysis bags containing precisely defined amounts of Opt-APG-AgNPs or apigenin suspension (control) were submerged in 25 mL of Phosphate-Buffered Saline (PBS, pH 7.4) while being continuously stirred at 150 rpm. To maintain sink conditions, 2 mL samples were removed at predefined intervals (0.5, 1, 2, 4,

IN PRESS

www.ijper.org

6, 8, and 24 h) and replaced with an equivalent volume of fresh PBS. A UV-visible spectrophotometer was used to measure the amount of released APG, and the mean±SD of three (n=3) trials was used to estimate the cumulative drug release.[25]

Radical Scavenging Assay by DPPH

The 2,2-Diphenyl-1-Picrylhydrazyl (DPPH) radical scavenging experiment was used to measure the Opt-APG-AgNPs' antioxidant activity. Apigenin suspension and Opt-APG-AgNPs were assessed at concentrations between 5 and 100 µg/mL. In short, 750 µL of newly made DPPH solution (0.02 g DPPH dissolved in 50 mL methanol) was combined with 750 µL of each sample. The positive control was ascorbic acid (20 µg/mL), and the negative control was methanol combined with DPPH solution. To stop photodegradation, the reaction mixtures were incubated in the dark for 30 min at 37°C. A UV-visible spectrophotometer was used to detect the absorbance at 517 nm following incubation. The following formula was used to determine the antioxidant activity, which was represented as the percentage of DPPH radical scavenging.[26]

$$\% \text{ Scavenging} = \frac{\text{OD of control} - \text{OD of sample}}{\text{OD of control}} \times 100$$

Preparation of Gel Formulation

To achieve a homogenous dispersion, carbopol 940 was dissolved in 100 mL of distilled water and left to hydrate for 2 hr at room temperature. After 60 min of stirring the hydrated polymer at 800 rpm, triethanolamine was gradually added until the pH was corrected and a clear, uniform gel was formed.[27] To guarantee even dispersion of the nanoparticles throughout the gel matrix, the Opt-APG-AgNPs were then added to the Carbopol gel base using a mechanical mixer running at 25 rpm for 2 min.[28]

Evaluation of Opt-APG-AgNPG

Physical characteristics of the created gel, including its color, appearance, consistency, pH, viscosity, and homogeneity, were also assessed.

Spreadability

The Opt-APG-AgNPG was measured to have a mass of up to 0.5 g and thereafter positioned on a glass-coated graph paper. Subsequently, an additional glass is positioned atop the mass of prepared gel. The diameter of the produced gel was ascertained by measuring the lengths of various sides. Subsequently, a supplementary load of 150 g was introduced, following which the combination was left undisturbed for a duration of 1 min. Then, the diameter of prepared gel was measured.[29]

IN PRESS

www.ijper.org

Table 2: Experimental response values by the BBd for the optimization of APG-AgNPs using Design Expert Software.

Run	A: $AgNO_3$ (mM)	B: Drug conc. (mg)	C: Microwave power (watt)	Y_1: particle size (nm)	Y_2: Absorbance
1	10	15	200	225.31	0.872
2	10	10	400	180.91	0.814
3	15	10	200	298.71	1.43
4	5	10	600	175.33	0.763
5	10	5	200	171.32	0.453
6	10	10	400	175.32	0.851
7	10	10	400	182.32	0.896
8	10	5	600	155.11	0.711
9	15	5	400	190.65	0.791
10	5	15	400	114.66	0.487
11	5	10	200	112.55	0.199
12	10	10	400	181.72	0.887
13	15	15	400	243.76	1.26
14	5	5	400	96.72	0.251
15	10	10	400	180.42	0.891
16	15	10	600	210.65	0.997
17	10	15	600	213.71	0.891

Viscosity

The viscosity of the Opt-APG-AgNPG formulations that were created was evaluated by employing a digital Brookfield viscometer (V420001, Fungi Lab, Sant Feliu Llobregat, Spain). The gel formulations were introduced into the sample container of the viscometer and placed untouched for a duration of 5 min to allow for settling. The viscosity of the substance was measured by employing the spindle, which was rotated at 50 Revolutions Per Minute (rpm) under a temperature of 25°C. The study was conducted at Centipoise (cP) in triplicate.[30]

Determination of drug content

To evaluate the consistency of drug distribution, the drug content of the Opt-APG-AgNPG was ascertained. The gel was centrifuged for 20 min at 1000 rpm after being diluted 100 times with deionised water (1:100, w/v) and vortexed for 5 min. A UV-visible spectrophotometer was used to analyse the supernatant at the specified wavelength, and the calibration curve was used to determine the drug content. Every measurement was done in triplicate and reported as mean±SD.[31]

Texture analysis

TA.XT Plus Texture Analyser (Stable Micro Systems Ltd., Surrey, UK) and the back-extrusion technique was used, the texture characteristics of the Opt-APG-AgNPG were assessed. A 100 mL beaker was filled with about 50 g of gel to ensure that there were no trapped air bubbles. The probe was set up to go at a steady pace of 2 mm/s through the gel to a depth of 15 mm. The instrument's software was used to record the texture characteristics after two successive compression cycles with a 20-sec gap between observations.[32,33]

Ex vivo permeation

A Franz diffusion cell was used to assess the *ex vivo* skin penetration of the Opt-APG-AgNPG and traditional apigenin gel (APG-CFG). With the stratum corneum facing the donor and the dermal side facing the receptor, excised skin was positioned between the donor and receptor compartments. Ten millilitres of Phosphate-Buffered Saline (PBS, pH 7.4) were added to the receptor chamber, which was kept at 37±0.5°C with constant magnetic stirring at 400 rpm. To maintain sink conditions, 2 mL aliquots were removed from the receptor compartment at predefined intervals (0.5, 1, 2, 4, 6, 8, and 24 hr) and promptly replaced with an equal volume of fresh PBS.

To find the total amount of apigenin penetrated, the collected samples were filtered, suitably diluted, and examined at 270 nm using a UV-visible spectrophotometer. Every experiment was conducted in triplicate, and the mean±SD is used to express the results.[34,35]

CLSM

CLSM was used to identify the qualitative absorption of silver nanoparticles by skin. To measure cellular uptake, rhodamine-B dye was mixed with the Opt-AgNPG formulation. The depth of penetration into skin of rat was measured by CLSM and compared to a control (a hydroalcoholic solution of rhodamine B). "Franz diffusion cells" were used in the CLSM experiment to conduct an 8-hr *ex vivo* research on skin penetration. A 488 nm confocal microscope was used to view the slides, which had a vertical stratum corneum. The wavelength at which the argon laser fluoresced was greater than 560 nm. The intensity of skin fluorescence in various layers was measured using confocal laser scanning microscopy (Leica TCS SPE (UK).[36]

Dermatokinetic

Excised rat skin mounted on a Franz diffusion cell was used for dermatokinetic investigations using the same experimental setup as the *ex vivo* permeation study. The donor compartment was treated with Opt-APG-AgNPG and APG-CFG. The skin was removed at predefined intervals (0.5, 1, 2, 4, 6, and 8 hr), thoroughly cleaned three times with distilled water to remove any remaining formulation, and submerged in water kept at 60°C to help separate the dermis and epidermis. To retrieve the medication, each layer of skin was sliced into tiny pieces and removed for 24 hr using 5 mL of ethanol. A 0.45 µm membrane filter was used to filter the extracts, and a UV-visible spectrophotometer set to a specific wavelength was used to measure the APG level. All experiments were carried out in (n=3), and the results were expressed as mean±SD.[37]

Stability studies

For six months, the stability of Opt-APG-AgNPs was assessed at accelerated circumstances (40±2°C /75±5% RH). To ascertain formulation stability, samples taken at 0, 30, 90, and 180 days were evaluated for particle size, PDI, zeta potential, phase separation, gel appearance, pH, homogeneity, spreadability, and drug content.

Statistical analysis

All data are expressed as mean±SD (n=3). Statistical comparisons were performed using one-way ANOVA, two-way ANOVA or an unpaired two-tailed Student's t-test, as appropriate. Tukey's post hoc test was applied for multiple comparisons. Analyses were conducted using GraphPad Prism version 6.0, and $p<0.05$ was considered statistically significant.

IN PRESS

www.ijper.org

RESULT AND DISCUSSION

APG-AgNPs - Optimization

The Box-Behnken design was used to evaluate the effects of $AgNO_3$ concentration, APG concentration and microwave power on particle size and absorbance. The design generated 17 experimental runs, including five centre-point runs, as presented in Table 2. The statistical parameters used to evaluate the fitted response models are summarized in Table 3. In order to assess the chosen model's relevance and determine the terms influencing the independent variable, the ANOVA was also used. Table 3 displays the R^2, standard deviation, and % Coefficient of Variation (CV) data pertaining to both responses. The F-values in this Table 3 show how significant the impact of each variable and how they interact with one another was on the response under consideration. Model terms with $p<0.05$ were considered statistically significant.[38] The quadratic models for particle size and absorbance were significant $p<0.0001$. The predicted-versus-actual plots showed close agreement between the experimental and model-predicted values for particle size and absorbance (Figure 2). This agreement, together with the high (R^2), adjusted (R^2) and predicted (R^2) values reported in Table 3, supported the adequacy of the fitted quadratic models. However, the plots represent model fit rather than validation using an independent experimental batch. The three-dimensional graph shows the relationship between several factors and particle size (nm) absorbance (Figure 1a and 1b).

Particle Size (Y_1): Effect of independent variables

Particle size= +180.14 + 55.56A+ 21.72B - 6.62C + 8.79AB - 37.71AC + 1.12BC -6.61 A^2 -12.08 B^2 + 25.78C^2

According to the polynomial equation, microwave power (C) had a negative impact on particle size, while $AgNO_3$ concentration (A) and APG concentration (B) had a positive impact (Figure 1a). Larger nanoparticles were formed when the concentration of $AgNO_3$ increased. The increased availability of Ag^+ ions, which encourages nanoparticle growth and increases particle diameter, is probably the cause of this behaviour. Furthermore, a red shift in the Surface Plasmon Resonance (SPR) band, which indicates the creation of bigger silver nanoparticles, is linked to higher $AgNO_3$ concentrations. On the other hand, when microwave power

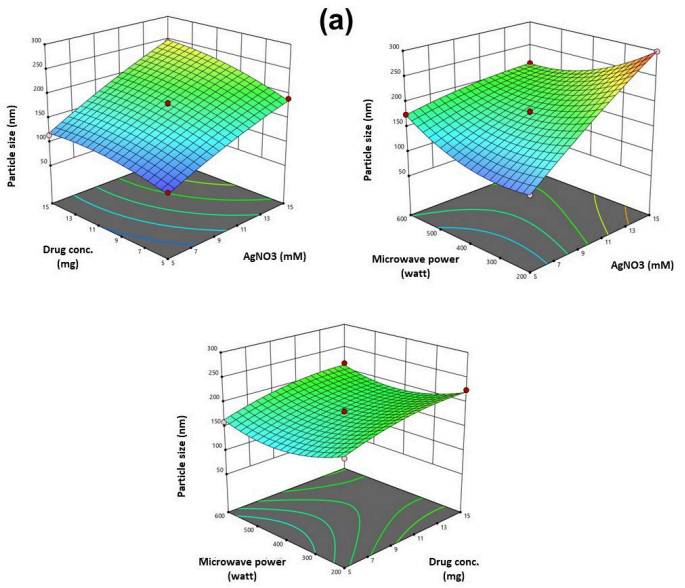


Figure 1a: 3D response surface plots,microwave power (C), apigenin concentration (B), and silver nitrate concentration (A) interact with nanoparticle size (Y_1, nm).[41].

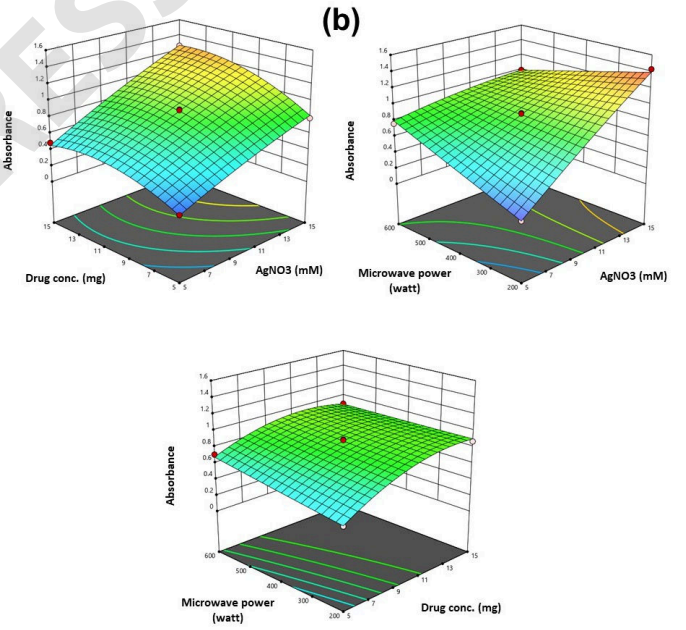


Figure 1b: 3D Response surface plots, microwave power (C), APG concentration (B), and $AgNO_3$ concentration (A) affect absorbance (Y_2).[41]

Table 3: Statistical parameters.

Responses	Analysis	R^2	Adjusted R^2	Predicted R^2	SD	%CV	Model	F value	*p* value
Particle size (nm)	Polynomial	0.9959	0.9906	0.9461	4.74	2.58	Quadratic Adequate precision= 56.71	50.83	< 0.0001
Absorbance	Polynomial	0.9925	0.9828	0.9248	0.0412	5.21	Quadratic Adequate Precision= 37.65	19.25	< 0.0001

IN PRESS

www.ijper.org

increased, nucleation was expedited and particle development was constrained, resulting in the creation of smaller nanoparticles.[39] Similar to this, apigenin concentration increased particle size by encouraging nanoparticle accumulation.[40] Nevertheless, the microwave's power exerted an adverse impact on the particle's dimensions, resulting in a reduction. Because a rise in surface area to volume ratio causes a drop in particle size, the nanoparticle's surface area is increased, which in turn promotes microwave absorption and makes the nanoparticles more effective. These findings are consistent with those found in earlier investigations.[40] Consequently, with a rise in the intensity of the microwave, there is a corresponding increase in absorption, while concurrently leading to a reduce in particle size.

Impact of independent variables on absorbance (Y_2)

$$\textbf{Absorbance}= +0.8768 + 0.3472A + 0.1630B + 0.0510C + 0.0582AB -0.2493\ AC -0.0597BC - 0.0320A^2 -0.1475B^2 + 0.0025C^2$$

According to the polynomial equation, absorbance was positively impacted by microwave power (C), APG concentration (B), and $AgNO_3$ concentration (A) (Figure 1a). Because higher Surface Plasmon Resonance (SPR) is linked to more Ag nanoparticle formation, raising the quantity of $AgNO_3$ from 5 to 15 mM improved the colour intensity and absorbance of the nanoparticle dispersion.[42] SPR is created when light interacts with Ag nanoparticles, resulting in distinctive optical absorption. While bigger particle size resulted in a red shift and broadening of the SPR absorption peak, higher Ag content enhanced colour intensity.[43,44] Higher absorbance values were obtained by increasing the apigenin concentration from 5 to 15 mg. This rise is explained by enhanced SPR, in which variations in the size and shape of nanoparticles cause a blue shift in the absorption spectrum and raise the absorbance intensity.[45] These findings are in line with previous studies.[18,40] In a similar manner, increase in microwave power causes decline in particle size causes change in SPR and causes increase in absorbance.

Validation of design

The outcome of the yield evaluation was discovered to be within the detection thresholds for the particle size (Y_1), and absorbance (Y_2) checkpoints. To validate the results were compared to the experimental and projected values of the response. The derived polynomial equation's reasonableness and the application of the BBD model were made easier by the modest percentage prediction error. Excellent goodness of fit was shown by the linear correlation plot between the actual and predicted values (p<0.0001) (Figure 2).

Optimized formulation

Numerical optimization predicted optimum conditions of 10.20 mM $AgNO_3$, 10.35 mg APG and 455.01 W microwave power. Among the 17 experimental runs, Batch 07, containing 10 mM $AgNO_3$ and 10 mg APG and prepared at 400 W, was selected for further characterization as the experimental formulation providing an acceptable balance between particle size and absorbance. In the subsequent sections, the term Opt-APG-AgNP refers to Batch 07 and not to a formulation prepared under the software-predicted conditions. An independent confirmation batch prepared under the numerically predicted conditions was not evaluated, which is acknowledged as a limitation of the optimization study.

IN PRESS

www.ijper.org

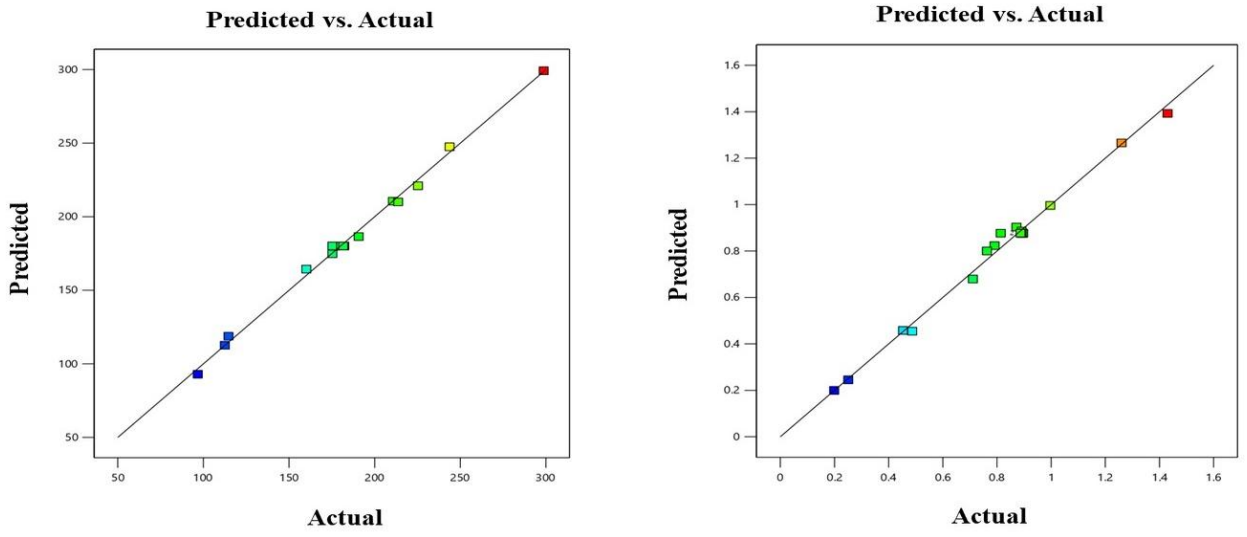


Figure 2: The predicted and observed graphical representations of the independent factors, namely $AgNO_3$ (A), drug concentration (B), and microwave power (C), in relation to the dependent variables, particle size (Y_1) and absorbance (Y_2).

Particle size, PDI and entrapment efficiency

DLS analysis showed that the optimized APG-AgNP formulation had a mean hydrodynamic diameter of 182.32 nm and a PDI of 0.244 (Figure 3). DLS measures the diameter of particles dispersed in a liquid medium, including the particle core and associated solvation layer. By expanding the surface area available for contact with the skin, the nanosized particles improve skin penetration and follicular deposition, which improves medication transport to the deeper epidermal and dermal layers.[46] The %EE of Opt-APG-AgNP was found to be 88.98%.

Zeta potential

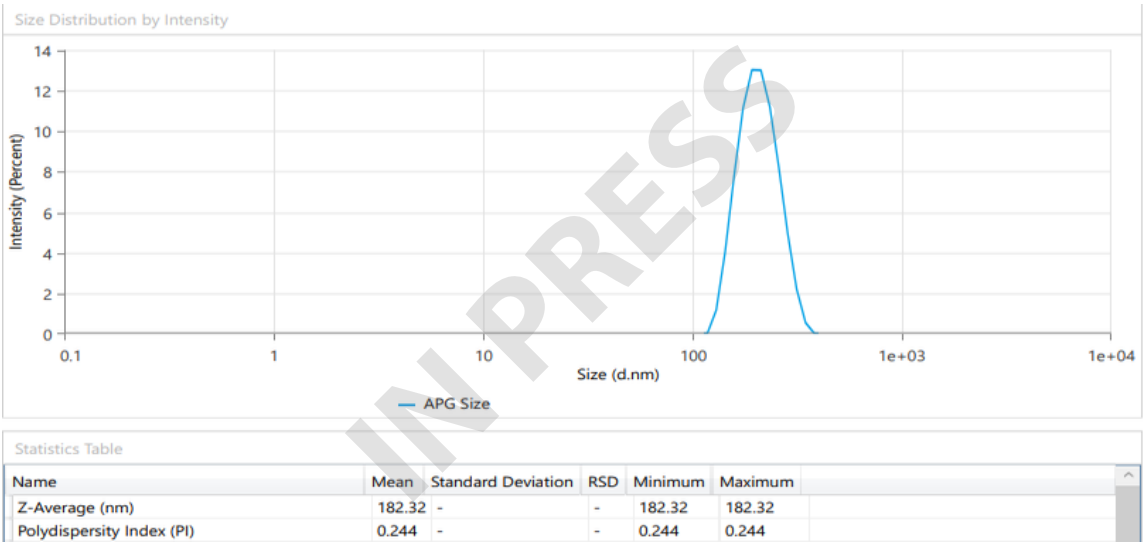
Both the stability of the particles and the interactions between the particles and the skin are heavily influenced by the charge of the formulation, which shows a significant effects in both aspects. The assessment of a colloidal system's stability can be conducted by considering the magnitude of its zeta potential. In scattered systems, electrostatic stability requires the maintenance of zeta potential falls between -35 and -25 mV.[47] As seen in Figure 4, the zeta potential of Opt-APG-AgNP was found to be -34.29 mV, suggesting its greater stability.[48]

TEM

TEM showed approximately spherical APG-AgNPs in the dried state (Figure 5). TEM provides information about particle morphology and core dimensions,[49] whereas DLS measures hydrodynamic diameter in dispersion; therefore, differences between the two measurements are expected.

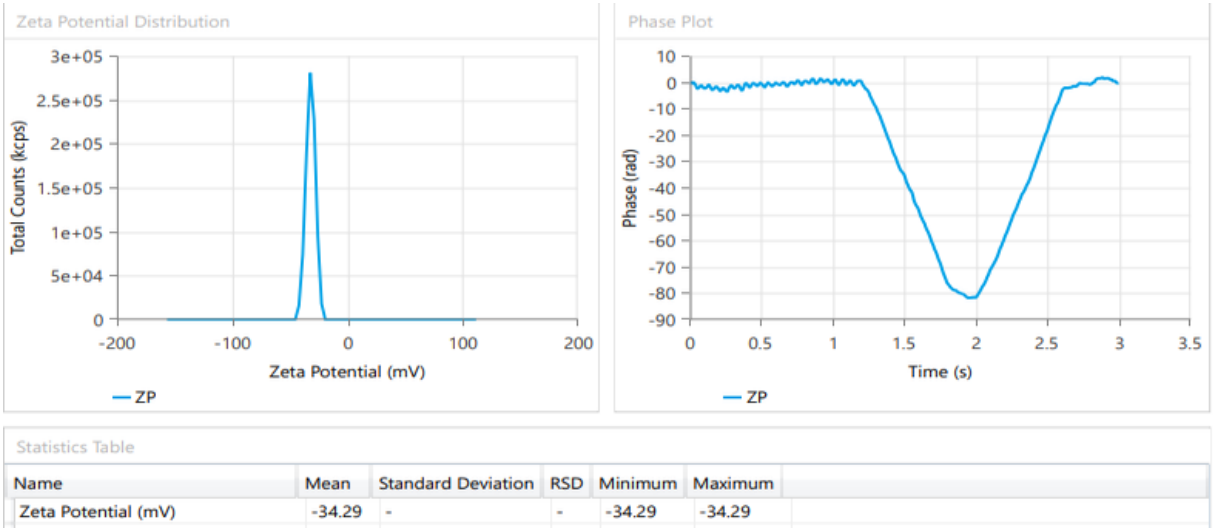
Drug release

The Opt-APG-AgNPs exhibited a considerably greater cumulative drug release (80.44±3.99%) in the *in vitro* release profile



Name	Mean	Standard Deviation	RSD	Minimum	Maximum
Z-Average (nm)	182.32	-	-	182.32	182.32
Polydispersity Index (PI)	0.244	-	-	0.244	0.244

Figure 3: Hydrodynamic particle-size distribution and PDI of the optimized APG-AgNP formulation determined by DLS.



Name	Mean	Standard Deviation	RSD	Minimum	Maximum
Zeta Potential (mV)	-34.29	-	-	-34.29	-34.29

Figure 4: Zeta-potential distribution of the optimized APG-AgNP formulation.

IN PRESS

www.ijper.org

compared to the APG solution (51.88±2.98%) (Figure 6).[50] The formulation exhibited a biphasic release pattern, with an initial burst during the first 5 hr followed by sustained release.[51] Diffusion of the encapsulated medication causes the sustained phase, whereas surface-associated APG is responsible for the first burst. According to kinetic analysis, the release behaviour was best represented by the Higuchi model (R^2= 0.9652), suggesting diffusion-controlled release. A non-Fickian (anomalous) diffusion mechanism was further validated by the Korsmeyer-Peppas model (R^2=0.9832, n=0.6984).[18,50]

Antioxidant activity

Prolonged exposure to damaging oxidants generates free radicals, which cause inflammatory changes in the skin. Antioxidant deficiencies increase the skin's vulnerability to oxidative stress, which can cause psoriatic inflammation.[52] The apigenin solution, opt-APG-AgNP formulation and ascorbic acid, were compared and investigated. The antioxidant activity, expressed as the percentage of scavenging, was found to be 92.79±1.74% for the reference solution containing ascorbic acid, 62.29±3.09% for the APG solution, and 82.26±2.56% for the optimized formulation of AGP-AgNP as shown in Figure 7. The anti-inflammatory actions elicited by apigenin are likely ascribed to its antioxidant characteristics. Apigenin is widely recognized as a potent antioxidant.[53] The data indicates that the use of Opt-APG-AgNP resulted in a significantly more pronounced impact compared to the use of APG solution in terms of lowering free radicals. The improved antioxidant activity of silver nanoparticles played a role in removal of radicals by enhancing antioxidant potential of APG.[54] Antioxidants provide a protective efficacy against reactive oxygen species molecules, which are responsible for inducing oxidative stress.[55] The greater DPPH radical-scavenging activity of Opt-APG-AgNP compared with the APG solution demonstrates improved *in vitro* antioxidant performance. However, antioxidant activity alone does not establish anti-inflammatory or anti-psoriatic efficacy.

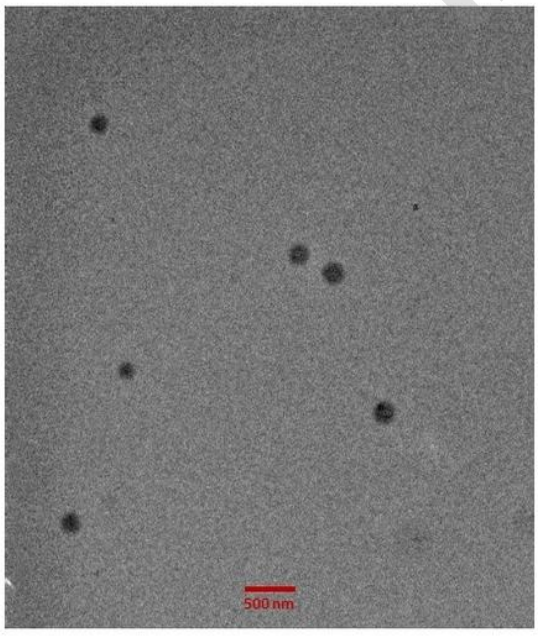


Figure 5: TEM micrograph showing the morphology of the optimized APG-AgNPs.

Evaluation of gel

The findings of the physical property evaluations of the produced Opt-APG-AgNPG. Considering that there were no particles that may be considered undesirable present throughout the procedure, the Opt-APG-AgNPG was uniform and visually pleasing. The gel that was produced had a pH of 5.99±0.23 and drug content 82.19%. With an extrudability of 20.21±1.14 g and a spreadability of 6.56 cm, the Opt-APG-AgNPG formulation shows that it can spread across the skin's surface with great ease, making it useful for topical administration. 2594.19 cps viscosity has reported of prepared gel. Viscosity is a fundamental property used to quantify the resistance of a fluid to flow, and it is commonly associated with the thickness of the fluid. In the context of gel formation, it pertains to fluids exhibiting a notably high viscosity range of 2000-4000 Centipoise (cps).[56]

Texture analysis

The produced topical Opt-APG-AgNPG formulation exhibited the following properties, according to software generated analysis: firmness (57.91g), cohesiveness (-31.77 g), consistency (42.67 g. sec), and cohesion work (-27.67 g.sec). Figure 8 displays the texture analysis profile that the software produced. The greatest (peak) force was used to measure firmness; greater results indicated a formulation that was more firm. The measurement of uniformity is determined by the area of the curve up to a specific point. A higher number indicates a thicker consistency of the sample. The presence of a (-) zone on the graph, observed during the return of the probe, can be attributed to the upward force exerted by the sample's weight predominantly on the upper surface of the disc. This phenomenon, known as back extrusion, provides valuable insights into the sample's consistency and its ability to resist flow off the disc. By taking into account the largest negative force, one can determine the level of cohesion within a sample.A higher magnitude of negativity in this value suggests a greater level of cohesion within the sample. The region beneath the curve with negative values can be denoted as the "work of cohesion." In other words, a larger numerical value in this region signifies a greater resistance of the sample to withdrawal. This resistance is indicative of the sample's cohesiveness, as well as its consistency.[57]

IN PRESS

www.ijper.org

Ex vivo permeation study

The findings of the skin penetration research, as shown in Figure 9, showed that the largest concentration of medication permeated the skin from Opt-APG-AgNPG, in contrast to standard gel formulation. A comparison of the permeation profiles of Opt-APG-AgNPG and APG-CFG revealed that 265.09±4.98 μg/cm^2, and 131.77±3.49 μg/cm^2 of drug penetrated the skin, respectively. The reported behaviour may be explained by the nanoparticles' smaller size and higher surface-to-volume ratio.[58] Upon simultaneous examination of the permeation characteristics, it was shown that the permeation exhibited a significant increase (p<0.0001). The permeability profile of the silver nanoparticles exhibited superior characteristics, with a flux rate of 10.00 μg/cm^2/hr. In contrast, the APG-CFG demonstrated a significantly lower flux rate of 5.10 μg/cm^2/hr, highlighting the notable disparity between the two formulations. This phenomenon may be attributed to the enhanced skin permeability resulting from the application of Carbopol-940, as well as the presence of nanometric particles, which further facilitated this process.[59] The results indicate that the Opt-APG-AgNPG formulation serves as an effective topical nano-drug delivery method, effectively impeding drug absorption through the skin over an extended duration and impeding its access to the systemic circulation. Compared to the conventional apigenin gel, the Opt-APG-AgNP gel showed much higher cumulative apigenin penetration and flux. The enhanced surface area available for skin engagement and the size of the nanometric particles may be linked to this improvement. These results show

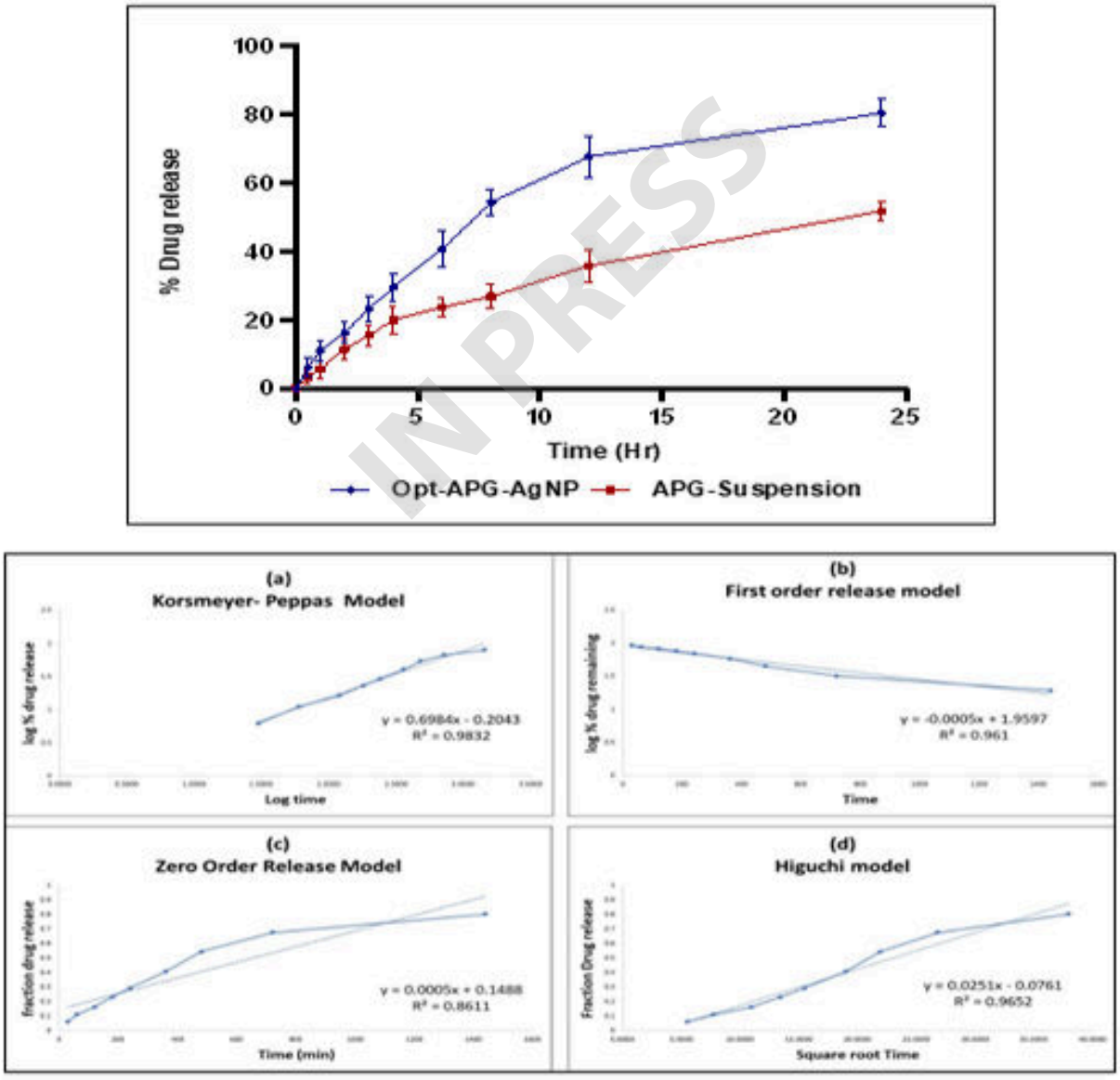


Figure 6: Comparative % drug release of APG-AgNP and APG-suspension (n=3, mean±SD, **p<0.0001) and kinetics models (a) Korsmeyer-Peppas, (b) First order release, (c) Zero order release, (d) Higuchi model of optimized apigenin loaded silver nanoparticles.

IN PRESS

www.ijper.org

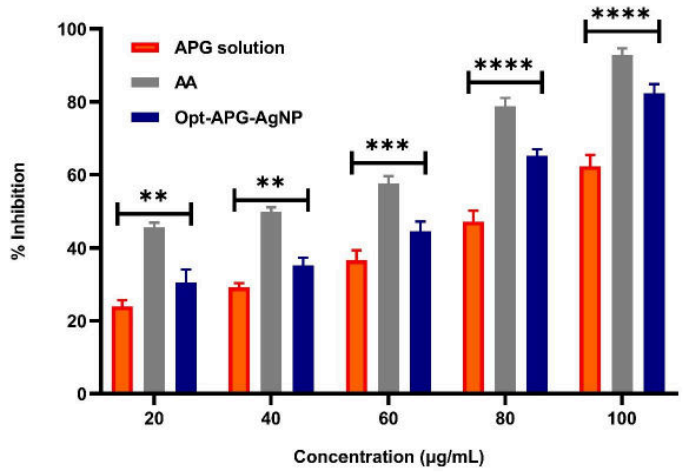


Figure 7: Concentration-dependent DPPH radical-scavenging activity of APG solution, Opt-APG-AgNP and ascorbic acid. Data are expressed as mean±SD (n=3). Statistical comparisons were performed using two-way ANOVA followed by Tukey's multiple-comparison test. Brackets represent comparisons between APG solution and Opt-APG-AgNP. **p<0.01, ***p<0.001 and ****p<0.0001.

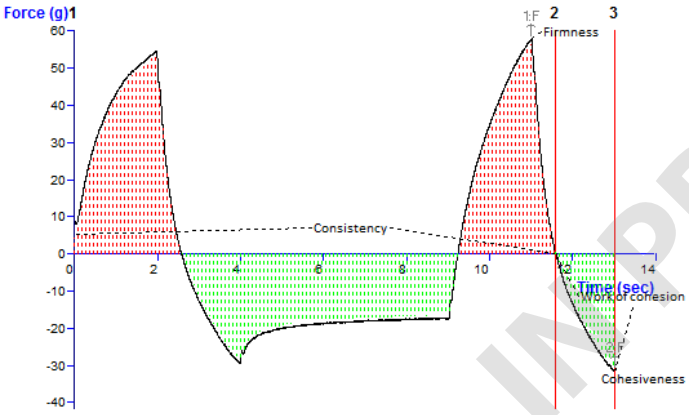


Figure 8: Texture analysis of Opt-APG-AgNPG.

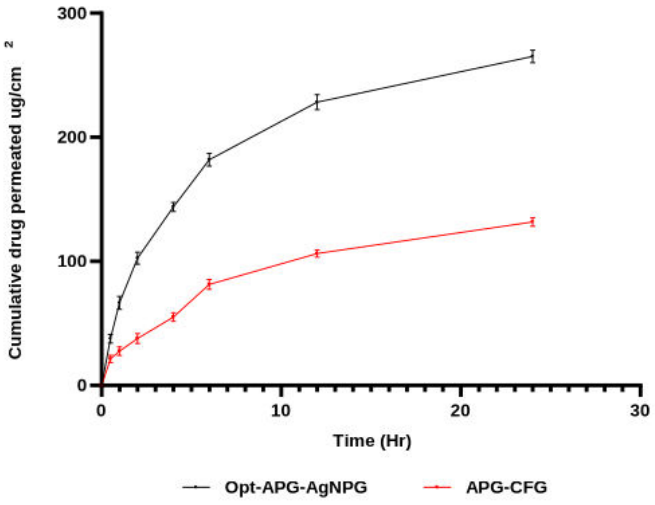


Figure 9: *Ex vivo* cumulative drug penetration comparison between APG-AgNPG and APG-CFG (n=3, mean±SD, **p<0.0001).

improved *ex vivo* apigenin distribution through removed skin. However, the current study did not assess systemic absorption, clinical effectiveness, or the decrease of systemic adverse effects.[58]

CLSM

The hydroalcoholic solution of rhodamine B demonstrated little penetration into the superficial skin layers, with fluorescence only observed up to a depth of around 15 µm (Figure 10a), according to CLSM (Figure 10). On the other hand, the optimised AgNP gel loaded with rhodamine B (Opt-AgNPG) penetrated the skin more deeply, reaching approximately 25 µm (Figure 10b). The nanoscale particle size, which expands the surface area and promotes better skin penetration, is probably the cause of this increased penetration.

Dermatokinetic study

The concentration of APG in the dermis and epidermis following an application of Opt-APG-AgNP gel and APG-CFG is shown in Figures 11a and 11b. Compared to the conventional formulation (APG-CFG), Opt-APG-AgNPG demonstrated a significantly greater (p<0.05) topical distribution of APG into the epidermal layers. Due to the increased drug penetration and retention through the epidermis, the $C_{Skin\ max}$ of the Opt-APG-AgNPG (184.31±5.59 µg/mL) was higher than that of the APG-CFG (111.66±1.59 µg/mL) based on dermatokinetics values. In addition, the Opt-APG-AgNPG $C_{skin\ max}$ was greater in the dermis (204.05±4.99 µg/cm^2) and (102.12±5.01 µg/cm^2) than it was in the APG-CFG formulation. In the epidermis and dermis, the Opt-APG-AgNPG AUC_{0-}^{8h} values were (1203.02±3.49 µg/cm^2/h) and (1226.64±4.18 µg/cm^2/h), respectively; the APG-CFG values were (647.98±2.97 µg/cm^2/h) and 577.69±1.29 µg/cm^2/h). The results unequivocally show that Opt-APG-AgNPG prolonged the drug's residence time in the dermis and epidermis, significantly lowered T_{max} (2 hr), and increased AUC in the dermis as well as C_{max} in both layers. These results validate the Opt-APG-AgNP gel's potential as an improved topical administration system by showing that it increased the epidermal and dermal deposition of apigenin in comparison to the standard gel. However, greater skin deposition does not prove anti-psoriatic effectiveness on its own. However, the dermatokinetic analysis was based on three experimental replicates, which limits statistical power and generalizability. These findings should therefore be considered preliminary and require confirmation in a larger study.

Stability studies

The stability studies result showed there were no major changes in the Opt-APG-AgNP and Opt-APG-AgNPG formulation at ambient temperature and humidity conditions (as per ICH) as depicted in Tables 4 and 5.

IN PRESS

www.ijper.org

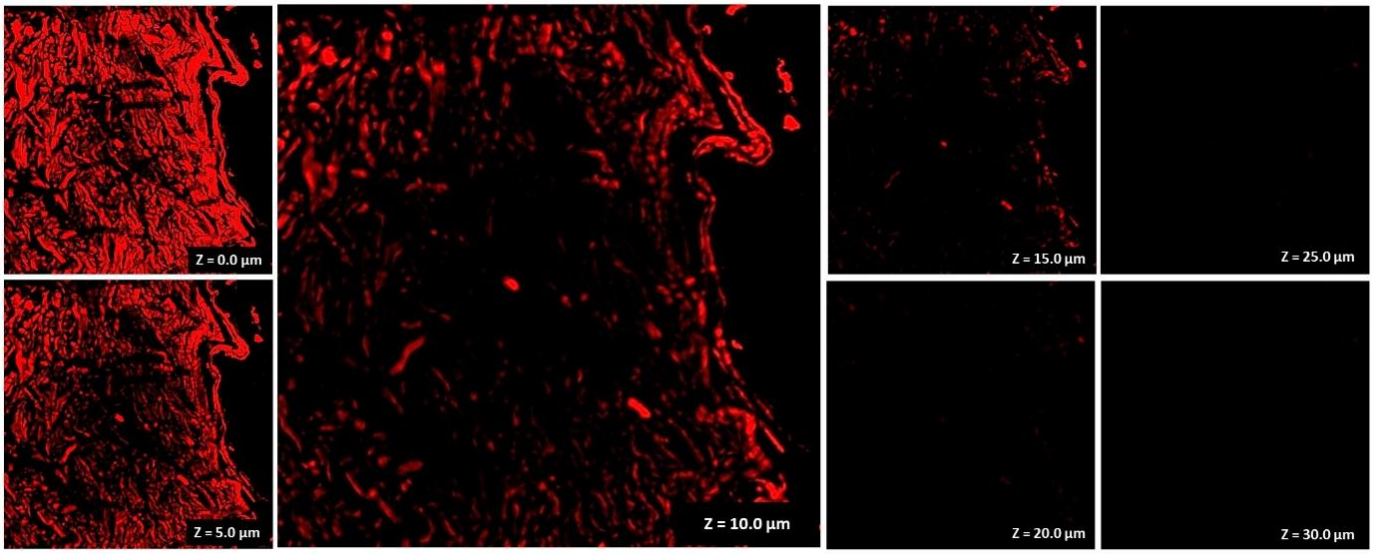


Figure 10: Comparative CLSM images of (a) standard solution and (b) opt-APG-AgNP.

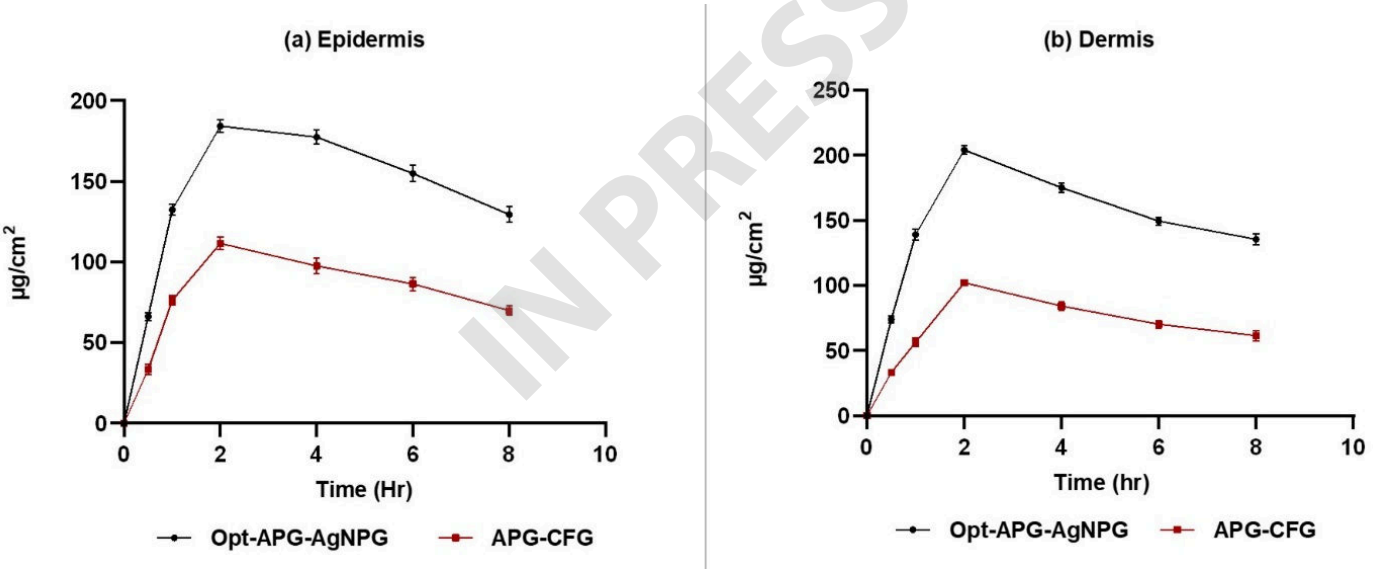


Figure 11: Comparative dermatokinetics analysis of Opt-APG-AgNPG and APG-CFG in (a) epidermis and (b) dermis (n=3, mean±SD, *p<0.05).

Table 4: Stability studies of Opt-APG-AgNP formulation.

Evaluation Parameters	Initial	30 days		90 days		180 days	
			40±2°C / 75±5% RH		40±2°C / 75±5% RH		40±2°C / 75±5% RH
Phase separation	No separation						
PDI	0.244		0.250		0.259		0.260
Particle size (nm)	182.32		185.78		190.13		199.24
Zeta potential (mV)	-34.32		-34.99		-37.47		-38.99

IN PRESS

www.ijper.org

Table 5: Stability studies of Opt-APG-AgNPG formulation.

Evaluation Parameters	Initial	30 days	90 days	180 days
		40±2°C /75±5% RH	40±2°C /75±5% RH	40±2°C /75±5% RH
Homogeneity	Homogeneous			
Clarity	Clear			
pH	5.99±0.45	6.14±0.67	6.09±5.17	6.19±0.78
Drug Content (%)	82.19±2.44	81.99±1.97	81.44±1.49	79.77±2.97

CONCLUSION

Using a Box-Behnken design, the apigenin-loaded silver nanoparticle formulation was effectively refined and added to a Carbopol 940 gel. Compared to the apigenin solution, the improved formulation showed better antioxidant activity, sustained drug release, and appropriate physicochemical and topical application qualities. In comparison to the traditional gel, *ex vivo* permeation, CLSM, and dermatokinetic investigations showed enhanced skin penetration and increased apigenin deposition in the epidermis and dermis. These results corroborate the APG-AgNP gel's promise as an improved topical apigenin delivery method. However, topical safety and psoriasis-specific treatment efficacy were not directly assessed in this investigation. To evaluate skin irritation, toxicity, inflammatory indicators, and anti-psoriatic efficacy, more *in vivo* research is necessary. Furthermore, the formulation's functional stability following storage was not thoroughly evaluated. Future stability investigations should include a stability-indicating assay to assess rheological behavior, drug-release kinetics, skin-permeation efficacy, entrapment efficiency, and potential apigenin degradation or leakage.

ACKNOWLEDGEMENT

None.

ABBREVIATIONS

AgNP: Silver nanoparticle; **$AgNO_3$:** Silver nitrate; **ANOVA:** Analysis of variance; **APG:** Apigenin; **APG-AgNP:** Apigenin-loaded silver nanoparticle; **APG-CFG:** Conventional apigenin gel formulation; **AUC:** Area under the curve; **BBD:** Box-Behnken design; **CLSM:** Confocal laser scanning microscopy; **COX-2:** Cyclooxygenase-2; **CV:** Coefficient of variation; **DLS:** Dynamic light scattering; **DPPH:** 2,2-Diphenyl-1-picrylhydrazyl; **DoE:** Design of experiments; **EE:** Entrapment efficiency; **HPLC:** High-performance liquid chromatography; **ICH:** International Council for Harmonisation; **IL:** Interleukin; **MWCO:** Molecular weight cut-off; **Opt-APG-AgNP:** Optimized apigenin-loaded silver nanoparticle; **Opt-APG-AgNPG:** Optimized apigenin-loaded silver nanoparticle gel; **PBS:** Phosphate-buffered saline; **PDI:** Polydispersity index; **PEG:** Polyethylene glycol; **RH:** Relative humidity; **RPM:** Revolutions per minute; **SD:** Standard deviation; **SPR:** Surface plasmon resonance; **TEA:** Triethanolamine; **TEM:** Transmission electron microscopy; **TNF:** Tumor necrosis factor; **UV:** Ultraviolet; **WHO:** World Health Organization;

CONFLICT OF INTEREST

The authors declare that there is no conflict of interest.

FUNDING

This research did not receive any specific grant from funding agencies in the public, commercial, or not-for-profit sectors.

ETHICAL APPROVAL

Not applicable.

SUMMARY

This study developed and optimized an apigenin-loaded silver nanoparticle gel for enhanced topical delivery. The optimized nanoparticles exhibited nanometric particle size, satisfactory colloidal properties, sustained drug release and greater antioxidant activity than free apigenin. Incorporation into a Carbopol gel produced suitable properties for topical application. *Ex vivo* permeation, CLSM and dermatokinetic studies demonstrated improved skin penetration and greater apigenin deposition in the epidermis and dermis compared with the conventional gel. Although these findings support the formulation as a potential topical apigenin-delivery system, psoriasis-specific endpoints, including lesion severity, inflammatory cytokines and keratinocyte hyperproliferation, were not evaluated. Therefore, its topical safety and anti-psoriatic efficacy require confirmation in appropriate *in vivo* studies.

AVAILABILITY OF DATA AND MATERIALS

The data will be available from the authors upon reasonable request.

IN PRESS

www.ijper.org

AUTHORS CONTRIBUTION

H.A.M. and M.A.: Contributed to the conceptualization and study design. **H.A.M.:** Conducted the experiments, analyzed the data, and drafted the manuscript. **M.A.:** Contributed to data interpretation, manuscript review, and editing. Both authors read and approved the final version of the manuscript.

REFERENCES

1. Sala M, Elaissari A, Fessi H. Advances in psoriasis physiopathology and treatments: Up to date of mechanistic insights and perspectives of novel therapies based on innovative skin drug delivery systems (ISDDS). Journal of Controlled Release. 2016;239:182-202.
2. Rendon A, Schäkel K. Psoriasis pathogenesis and treatment. International journal of molecular sciences. 2019;20(6):1475.
3. W.H. Organization, Global report on psoriasis. World Health Organization, 2016.
4. Harden JL, Krueger JG, Bowcock AM. The immunogenetics of psoriasis: a comprehensive review. Journal of autoimmunity. 2015;64:66-73.
5. Menter A, Gottlieb A, Feldman SR, Van Voorhees AS, Leonardi CL, Gordon KB, *et al.* Guidelines of care for the management of psoriasis and psoriatic arthritis: Section 1. Overview of psoriasis and guidelines of care for the treatment of psoriasis with biologics. Journal of the American Academy of Dermatology. 2008;58(5):826-50.
6. Qadir A, Aqil M, Ali A, Warsi MH, Mujeeb M, Ahmad FJ, Ahmad S, *et al.* Nanostructured lipidic carriers for dual drug delivery in the management of psoriasis: Systematic optimization, dermatokinetic and preclinical evaluation. Journal of Drug Delivery Science and Technology. 2020;57:101775.
7. Panche AN, Diwan AD, Chandra SR. Flavonoids: an overview. Journal of nutritional science. 2016;5:e47.
8. Yoon JH, Kim MY, Cho JY. Apigenin: A therapeutic agent for treatment of skin inflammatory diseases and cancer. International Journal of Molecular Sciences. 2023;24(2):1498.
9. Elkhawaga OY, Ellety MM, Mofty SO, Ghanem MS, Mohamed AO. Review of natural compounds for potential psoriasis treatment. Inflammopharmacology. 2023;31(3):1183-98.
10. Waheed A, Zameer S, Sultana N, Ali A, Aqil M, Sultana Y, Iqbal Z. Engineering of QbD driven and ultrasonically shaped lyotropic liquid crystalline nanoparticles for Apigenin in the management of skin cancer. European Journal of Pharmaceutics and Biopharmaceutics. 2022;180:269-80.
11. Goyal R, Macri LK, Kaplan HM, Kohn J. Nanoparticles and nanofibers for topical drug delivery. Journal of Controlled Release. 2016;240:77-92.
12. Rehman MU, Yoshihisa Y, Miyamoto Y, Shimizu T. The anti-inflammatory effects of platinum nanoparticles on the lipopolysaccharide-induced inflammatory response in RAW 264.7 macrophages. Inflammation Research. 2012;61(11):1177-85.
13. Crisan M, David L, Moldovan B, Vulcu A, Dreve S, Perde-Schrepler M, Tatomir C, Filip AG, Bolfa P, Achim M, Chiorean I. New nanomaterials for the improvement of psoriatic lesions. J. Mater. Chem. B. 2013;1:3152-8.
14. Lademann J, Richter H, Teichmann A, Otberg N, Blume-Peytavi U, Luengo J, Weiss B, Schaefer UF, Lehr CM, Wepf R, Sterry W. Nanoparticles-an efficient carrier for drug delivery into the hair follicles. European journal of pharmaceutics and biopharmaceutics. 2007;66(2):159-64.
15. Murphy CJ. Sustainability as an emerging design criterion in nanoparticle synthesis and applications. Journal of Materials Chemistry. 2008;18(19):2173-6.
16. Wong KK, Cheung SO, Huang L, Niu J, Tao C, Ho CM, Che CM, Tam PK. Further evidence of the anti-inflammatory effects of silver nanoparticles. ChemMedChem: Chemistry enabling drug discovery. 2009;4(7):1129-35.
17. Banerjee J, Narendhirakannan RT. Biosynthesis of silver nanoparticles from *Syzygium cumini* (L.) seed extract and evaluation of their *in vitro* antioxidant activities. Dig J Nanomater Biostruct. 2011;6(3):961-8.
18. Ghazwani M, Hani U, Alqarni MH, Alam A. Development and characterization of methyl-anthranilate-loaded silver nanoparticles: A phytocosmetic sunscreen gel for UV protection. Pharmaceutics. 2023;15(5):1434.
19. Lalegani Z, Ebrahimi SS. Optimization of synthesis for shape and size controlled silver nanoparticles using response surface methodology. Colloids and Surfaces A: Physicochemical and Engineering Aspects. 2020;595:124647.
20. Zhang XF, Liu ZG, Shen W, Gurunathan S. Silver nanoparticles: synthesis, characterization, properties, applications, and therapeutic approaches. International journal of molecular sciences. 2016;17(9):1534.
21. Kaur A, Preet S, Kumar V, Kumar R, Kumar R. Synergetic effect of vancomycin loaded silver nanoparticles for enhanced antibacterial activity. Colloids and Surfaces B: Biointerfaces. 2019;176:62-9.
22. Bisht D, Verma D, Mirza MA, Anwer MK, Iqbal Z. Development of ethosomal gel of ranolazine for improved topical delivery: *in vitro* and *ex vivo* evaluation. Journal of molecular liquids. 2017;225:475-81.
23. Anjum F, Zakir F, Verma D, Aqil M, Singh M, Jain P, Mirza MA, Anwer MK, Iqbal Z. Exploration of nanoethosomal transgel of naproxen sodium for the treatment of arthritis. Current Drug Delivery. 2020;17(10):885-97.
24. Ravindra S, Mulaba-Bafubiandi AF, Rajinikanth V, Varaprasad K, Narayana Reddy N, Mohana Raju K. Development and characterization of curcumin loaded silver nanoparticle hydrogels for antibacterial and drug delivery applications. Journal of Inorganic and Organometallic Polymers and Materials. 2012;22(6):1254-62.
25. Todorova M, Milusheva M, Kaynarova L, Georgieva D, Delchev V, Simeonova S, Pilicheva B, Nikolova S. Drug-loaded silver nanoparticles—a tool for delivery of a mebeverine precursor in inflammatory bowel diseases treatment. Biomedicines. 2023;11(6):1593.
26. Ibraheem DR, Hussein NN, Sulaiman GM, Mohammed HA, Khan RA, Al Rugaie O. Ciprofloxacin-loaded silver nanoparticles as potent nano-antibiotics against resistant pathogenic bacteria. Nanomaterials. 2022;12(16):2808.
27. Singh S, Vardhan H, Kotla NG, Maddiboyina B, Sharma D, Webster TJ. The role of surfactants in the formulation of elastic liposomal gels containing a synthetic opioid analgesic. International journal of nanomedicine. 2016 Apr 8:1475-82.
28. Mirza MA, Ahmad S, Mallick MN, Manzoor N, Talegaonkar S, Iqbal Z. Development of a novel synergistic thermosensitive gel for vaginal candidiasis: an *in vitro, in vivo* evaluation. Colloids and Surfaces B: Biointerfaces. 2013;103:275-82.
29. Fatima M, Monawwar S, Mohapatra S, Alex TS, Ahmed A, Taleuzzaman M, Ali A, Ansari MJ, Mirza MA, Iqbal Z. *In silico* drug screening based development of novel formulations for onychomycosis management. Gels. 2021;7(4):221.
30. Nurman S, Yulia R, Irmayanti, Noor E, Candra Sunarti T. The optimization of gel preparations using the active compounds of arabica coffee ground nanoparticles. Scientia Pharmaceutica. 2019;87(4):32.
31. Fong Yen W, Basri M, Ahmad M, Ismail M. Formulation and evaluation of galantamine gel as drug reservoir in transdermal patch delivery system. The scientific world journal. 2015;2015(1):495271.
32. Tafuro G, Costantini A, Baratto G, Francescato S, Busata L, Semenzato A. Characterization of polysaccharidic associations for cosmetic use: Rheology and texture analysis. Cosmetics. 2021;8(3):62.
33. Zakir F, Ahmad A, Farooq U, Mirza MA, Tripathi A, Singh D, Shakeel F, Mohapatra S, Ahmad FJ, Kohli K. Design and development of a commercially viable *in situ* nanoemulgel for the treatment of postmenopausal osteoporosis. Nanomedicine. 2020;15(12):1167-87.
34. Nagaich U, Gulati N, Chauhan S. Antioxidant and antibacterial potential of silver nanoparticles: biogenic synthesis utilizing apple extract. Journal of pharmaceutics. 2016;2016(1):7141523.
35. Khan R, Mirza MA, Aqil M, Hassan N, Zakir F, Ansari MJ, Iqbal Z. A pharmaco-technical investigation of thymoquinone and peat-sourced fulvic acid nanoemulgel: A combination therapy. Gels. 2022;8(11):733.
36. Imran M, Iqubal MK, Imtiyaz K, Saleem S, Mittal S, Rizvi MM, Ali J, Baboota S. Topical nanostructured lipid carrier gel of quercetin and resveratrol: Formulation, optimization, *in vitro* and *ex vivo* study for the treatment of skin cancer. International journal of pharmaceutics. 2020;587:119705.
37. Negi P, Singh B, Sharma G, Beg S, Katare OP. Biocompatible lidocaine and prilocaine loaded-nanoemulsion system for enhanced percutaneous absorption: QbD-based optimisation, dermatokinetics and *in vivo* evaluation. Journal of microencapsulation. 2015;32(5):419-31.
38. Haque SK. Optimized and validated box-Behnken design combined response surface methodology to quantify acetic acid content in potassium clavulanate using high-performance liquid chromatography. Yanbu Journal of Engineering and Science. 2022;19(2):50-61.
39. Bamsaoud SF, Basuliman MM, Bin-Hameed EA, Balakhm SM, Alkalali AS. The effect of volume and concentration of AgNO3 aqueous solutions on silver nanoparticles synthesized using *Ziziphus Spina-Christi* leaf extract and their antibacterial activity. InJournal of Physics: Conference Series 2021;1900(1):012005. IOP Publishing.
40. Alam A, Foudah AI, Alqarni MH, Yusufoglu HS. Microwave-assisted and chemically tailored chlorogenic acid-functionalized silver nanoparticles of *Citrus sinensis* in gel matrix aiding QbD design for the treatment of acne. Journal of Cosmetic Dermatology. 2023;22(5):1613-27.
41. Makeen HA, Albratty M. Sesamol loaded silver nanoparticles gel engineered for wound healing via topical delivery: optimization *in vitro and ex vivo* evaluation. Current Pharmaceutical Design. 2024;30(40):3175-89.
42. Slistan-Grijalva A, Herrera-Urbina R, Rivas-Silva JF, Ávalos-Borja M, Castillón-Barraza FF, Posada-Amarillas A. Classical theoretical characterization of the surface plasmon absorption band for silver spherical nanoparticles suspended in water and ethylene glycol. Physica E: Low-dimensional Systems and Nanostructures. 2005;27(1-2):104-12.
43. Sobczak-Kupiec A, Malina D, Wzorek Z, Zimowska M. Influence of silver nitrate concentration on the properties of silver nanoparticles. Micro & Nano Letters. 2011;6(8):656-60.

IN PRESS

www.ijper.org

44. Bonnia NN, Ab Rani MA, Fairuzi AA. Study on parameters optimization of silver nanoparticles biosynthesized using aqueous extract of *Imperata cylindrica*. Desalination and Water Treatment. 2020;174:186-95.

45. Anandalakshmi K, Venugobal J, Ramasamy VJ. Characterization of silver nanoparticles by green synthesis method using *Pedalium murex* leaf extract and their antibacterial activity. Applied nanoscience. 2016;6(3):399-408.

46. Adib ZM, Ghanbarzadeh S, Kouhsoltani M, Khosroshahi AY, Hamishehkar H. The effect of particle size on the deposition of solid lipid nanoparticles in different skin layers: a histological study. Advanced pharmaceutical bulletin. 2023;6(1):31-6.

47. Nasr AM, Moftah F, Abourehab MA, Gad S. Design, formulation, and characterization of valsartan nanoethosomes for improving their bioavailability. Pharmaceutics. 2022;14(11):2268.

48. Erdogan O, Abbak M, Demirbolat GM, Birtekocak F, Aksel M, Pasa S, Cevik O. Green synthesis of silver nanoparticles via *Cynara scolymus* leaf extracts: The characterization, anticancer potential with photodynamic therapy in MCF7 cells. PloS one. 2019;14(6):e0216496.

49. Espinosa JC, Cerritos RC, Morales MA, Guerrero KP, Contreras RA, Macías JH. Characterization of silver nanoparticles obtained by a green route and their evaluation in the bacterium of *Pseudomonas aeruginosa*. Crystals. 2020;10(5):395.

50. Rozalen M, Sánchez-Polo M, Fernández-Perales M, Widmann TJ, Rivera-Utrilla J. Synthesis of controlled-size silver nanoparticles for the administration of methotrexate drug and its activity in colon and lung cancer cells. RSC advances. 2020;10(18):10646-60.

51. Su Z, Sun D, Zhang L, He M, Jiang Y, Millar B, Douglas P, Mariotti D, Maguire P, Sun D. Chitosan/silver nanoparticle/graphene oxide nanocomposites with multi-drug release, antimicrobial, and photothermal conversion functions. Materials. 2021;14(9):2351.

52. Briganti S, Picardo M. Antioxidant activity, lipid peroxidation and skin diseases. What's new. Journal of the European academy of dermatology and venereology. 2003;17(6):663-9.

53. Man MQ, Hupe M, Sun R, Man G, Mauro TM, Elias PM. Topical apigenin alleviates cutaneous inflammation in murine models. Evidence-Based Complementary and Alternative Medicine. 2012;2012(1):912028.

54. Keshari AK, Srivastava R, Singh P, Yadav VB, Nath G. Antioxidant and antibacterial activity of silver nanoparticles synthesized by *Cestrum nocturnum*. Journal of Ayurveda and integrative medicine. 2020;11(1):37-44.

55. Madhulatha M, Vijayabhaskar M. Evaluation of therapeutic efficacy of antioxidants in psoriatic cases. Indian Journal of Medical Biochemistry. 2019;23(1):167-9.

56. Danimayostu AA. Pengaruh penggunaan pati kentang (*Solanum tuberosum*) termodifikasi asetilasi-oksidasi sebagai gelling agent terhadap stabilitas gel natrium diklofenak. Pharmaceutical journal of Indonesia. 2017;3(1):25-32.

57. Somagoni J, Boakye CH, Godugu C, Patel AR, Mendonca Faria HA, Zucolotto V, Singh M. Nanomiemgel-a novel drug delivery system for topical application-*in vitro and in vivo* evaluation. PLoS One. 2014;9(12):e115952.

58. Sadozai SK, Khan SA, Baseer A, Ullah R, Zeb A, Schneider M. *In vitro, ex vivo, and in vivo* evaluation of nanoparticle-based topical formulation against *Candida albicans* infection. Frontiers in pharmacology. 2022;13:909851.

59. Noor A, Jamil S, Sadeq TW, Mohammed Ameen MS, Kohli K. Development and evaluation of nanoformulations containing timur oil and rosemary oil for treatment of topical fungal infections. Gels. 2023;9(7):516.

Cite this article: Makeen HA, Albratty M. Development and Optimization of an Apigenin-Loaded Silver Nanoparticle Gel for Enhanced Topical Delivery of Apigenin. Indian J of Pharmaceutical Education and Research. 2027;1-15.

IN PRESS

www.ijper.org